ELSEVIER

Thermochimica Acta 334 (1999) 131–139

thermochimica acta

www.elsevier.com/locate/tca

Carbochlorination of TiO_2

Julio Andrade Gamboa[a,*], Ana E. Bohé[b], Daniel M. Pasquevich[a]

[a]Comisión Nacional de Energía Atómica, Centro Atómico Bariloche, 8400 San Carlos de Bariloche, Río Negro, Argentina
[b]Consejo Nacional de Investigaciones Cientificas y Técnicas, Centro Atómico Bariloche, 8400 San Carlos de Bariloche, Río Negro, Argentina

Received 8 February 1999; received in revised form 1 June 1999; accepted 1 June 1999

Abstract

The kinetics of carbochlorination of TiO_2, using TiO_2(s)–carbon(s) powder mixtures and a flowing Ar(g)–Cl_2(g) reaction atmosphere, has been investigated as a function of two parameters: temperature (733–1223 K) and carbon content in the solid mixture. Carbochlorination of TiO_2 exhibits two well-differentiated and successive reaction stages. The first reaction stage occurs immediately and the second stage proceeds at a rate up to two orders of magnitude lower. For both reaction stages, the rate increases with carbon content. The first stage occurs under external chlorine transport control for high carbon contents and under internal mixed control for low carbon contents. The second reaction stage occurs nearly under chemical control at all carbon contents. © 1999 Elsevier Science B.V. All rights reserved.

Keywords: Titania; Carbochlorination; Kinetic; Gas–solid

---

1. Introduction

Gas–solid reactions represent an important subject of applied and theoretical investigations. These reactions are usually associated with industrial processes in which operation parameters need to be controlled. The overall kinetics need to be known, but in some cases it is necessary to know the reaction mechanism which may provide physical chemical criteria to enhance the industrial process.

The chlorination of metallic oxides in the presence of carbon (carbochlorination) is an example of gas–solid reactions of industrial importance. The mechanism is not well understood even though carbochlorination has been applied since 1940 as one step in the industrial extraction of Zr and Ti [1]. The carbochlorination stoichiometry at high temperatures (1023–1273 K) is represented by the following equation [2–6].

$$\begin{aligned} &MeO_2(s) + 2Cl_2(g) + 2C(s) \\ &\quad = MeCl_4(g) + 2CO(g) \end{aligned} \qquad (1)$$

where Me is Zr or Ti. The chlorination of ZrO_2 and TiO_2 is performed in the presence of carbon to make the formation of the respective chlorides thermodynamically favourable at all temperatures, since direct chlorination is not feasible. Carbon has a thermodynamic effect on the chlorination of oxides. It reduces the oxygen potential favouring chloride formation. Another reducing agent widely used to convert refractory oxides into their chlorides is CO, but it is known that chlorination of TiO_2 and other oxides under the

---

*Corresponding author. Fax: +54-2944445299
E-mail address: andrade@cab.cnea.gov.ar (J. Andrade Gamboa)

PII: S0040-6031(99)00141-0

same oxygen potential is faster in the presence of carbon than in the presence of CO [2,7–9]. Hence, carbon, in addition, has a kinetic effect and it has been suggested that carbon may be involved in the formation of active species for chlorination [2].

The carbochlorination mechanisms are incompletely understood. Most reports [2,6,8,10] have agreed that the contact between carbon and oxide particles is not necessary. Hence, it has been proposed that carbochlorination occurs via gaseous intermediates formed during reaction. Among them, phosgene (Cl_2CO) [3], chlorine atoms (Cl) [2,4,6,8,11] and oxychlorides [7] have been principally proposed, though these have not been detected experimentally. It has been proposed that formation of both phosgene [3] and chlorine atoms [12] take place on the carbon surface. Phosgene may be formed by an heterogeneous reaction of Cl_2 with CO, since CO is always initially adsorbed on carbon. Chlorine atoms may be formed by Cl_2 dissociation in the C–Cl_2 interaction. Hence, either in phosgene formation or in chlorine atom generation, the carbon surface is involved. The overall reaction rate may be proportional to carbon content in the sample since the carbon area increases and the intermediate concentration in the gaseous phase is enhanced. Dunn [7] found that varying carbon contents in TiO_2–C mixtures, the TiO_2 chlorination rate increases linearly up to about 25 wt% of carbon.

The kinetics of ZrO_2 carbochlorination using ZrO_2(s)–C(s) powder mixtures has been studied in our laboratory [4,13–17]. It has been shown [13,14] that this reaction involves two well-differentiated reaction stages. The rate of the first reaction stage is two or three orders of magnitude higher than that of the second reaction stage. This kinetic instability [18], has not been reported for other carbochlorination systems. The initial and the final reaction stages have been named "fast" and "slow" stages, respectively [13,14]. A detailed kinetic study [14,15] has shown that the rate controlling regime of the fast stage is mixed (chemical-internal diffusion) and the rate determining step of the slow stage is chemical in nature. Earlier studies [13,17] have suggested that chlorine atoms are the most probable reaction intermediate. In addition, the reaction is faster for 70 wt% of carbon than for 20 wt% of carbon. This suggests the participation of carbon in the formation of the reaction intermediates. However, if under certain conditions, a common mechanism could operate for different oxides is not known.

The aim of this work is to investigate the behaviour of the TiO_2 chlorination in the presence of carbon and the effect of carbon content on the chlorination rate.

2. Experimental

2.1. Procedure

The samples were prepared by mechanical mixing of TiO_2 and carbon powders. Both powders have been used in previous studies and they have been well characterized [4,13–17,19]. In particular, the carbon used in this work is the same used in ZrO_2 carbochlorination studies [4,13–17].

TiO_2 carbochlorination was studied using a thermogravimetric system adapted to work with corrosive atmospheres, which has been described elsewhere [13]. Samples ranging from 1 to 20 mg were placed in the thermogravimetric system in a quartz crucibles and maintained at working temperature for 1 h in flowing argon. Chlorine was injected in the argon flow (total flow 2.1 l/h NTP) at a maintaining the chlorine partial pressure of 0.35 atm (35 kPa). Mass changes and time were continuously measured with a data acquisition system. When a given mass change was obtained, the chlorine flow was cut off, the reaction stopped and the sample was cooled to room temperature within the equipment under flowing Ar. Experimental data were corrected taking into account apparent mass changes as previously reported [13]. The reproducibility in thermogravimetric curves is related to a deviation no greater than 5% [17].

The thermogravimetric runs were carried out at temperatures between 733 and 1223 K using the TiO_2–C powder mixtures with 2.5, 10, 30 and 70 wt% of carbon. Some reaction residues were also examined by scanning electron microscopy (SEM).

2.2. Expression of results

The reaction degree is given by $\alpha = \Delta m(TiO_2)/m_0(TiO_2)$, where $\Delta m(TiO_2)$ is the TiO_2 mass loss and $m_0(TiO_2)$ is the initial TiO_2 mass. From stoichiometry of reaction (1) $\Delta m(TiO_2) = 0.769\Delta M$, where ΔM is the observed mass change (carbon plus oxide). Therefore, reaction degree is

$$\alpha = -[0.769\Delta M/m_0(\mathrm{TiO_2})]. \tag{2}$$

The reaction rate is calculated as

$$\mathrm{R} = \mathrm{d}\alpha/\mathrm{d}t = -[0.769/m_0(\mathrm{TiO2})]\,(\mathrm{d}M/\mathrm{d}t)\ (\mathrm{s}^{-1}). \tag{3}$$

From Eq. (3) the reaction rate expressed as moles of Cl_2 reacted is

$$r = \mathrm{d}n(\mathrm{Cl_2})/\mathrm{d}t = [2m_0(\mathrm{TiO_2})/\mu(\mathrm{TiO_2})]R \times (\mathrm{moles\,Cl_2/s}),$$

where $n(Cl_2)$ are moles of Cl_2 and $\mu(TiO_2)$ is the formula weight of TiO_2. Initial reaction rates (at $t = 0$) are denoted with subscript 0.

3. Results

3.1. Thermogravimetry

Fig. 1 shows the relative mass changes as a function of time obtained at 1223 K during chlorination of pure carbon (a) pure TiO_2 (b) and TiO_2–30 wt% C mixture (c). Curve (a) shows that when chlorine was introduced, carbon underwent a mass gain of approximately 8% initially. Subsequently, a slow and continuous mass loss occurred. After 2 h, the net mass gain was about 2%. Curve (b) shows that the chlorination of TiO_2 involves a slow and linear mass loss which became about 25% of the initial mass after 100 min of reaction. Curve (c) clearly shows that TiO_2–C mixture rapidly reacted with chlorine achieving a reaction degree (α) of 0.28 and nearly 0.90 after first 5 and 100 min of reaction, respectively. In the last curve, two zones of reaction were observed: a linear zone in the first 5 min and a decreasing mass loss thereafter.

The behaviour shown in curve (c) of Fig. 1 is a characteristic of TiO_2 carbochlorination under certain experimental conditions. This is better illustrated in Fig. 2, which shows the relative mass changes ($\Delta M/m_0(TiO_2)$) corresponding to the chlorination of a TiO_2–10 wt% C mixture at 1073 K. The thermogravimetric curve exhibits two well-differentiated reaction stages: the first one, with a fast mass change during a short time, and the second one with a slower mass change. From the slope of the first stage and using Eq. (3), the initial reaction rate, $R_{0,\mathrm{f}}$, was calculated. The extension of the first reaction stage, (the reaction degree, α_f), was computed using Eq. (2) from curves $\Delta M/m_0(TiO_2)$ vs. time as the ordinate of intersection of linear extrapolations of the two stages, as shown in Fig. 2.

Fig. 3 shows the effect of temperature on the chlorination of TiO_2–70 wt% C mixture. Similar behaviour, as shown in Fig. 2, was observed between 923 and 1073 K. When temperature was decreased from 1073 to 923 K, the mass fraction chlorinated during the first

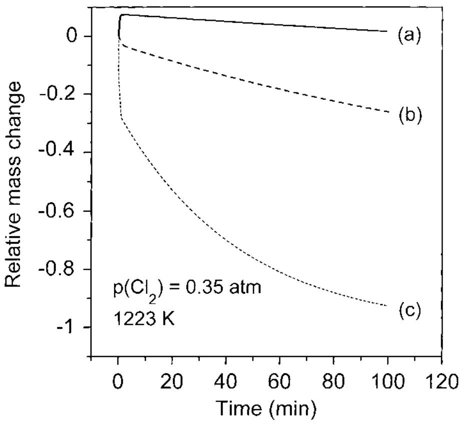

Fig. 1. Relative mass changes as a function of time corresponding to experiments of chlorination at 950°C of (a) carbon, (b) TiO_2 and (c) TiO_2–30 wt% C mixture. In case (c), mass changes are relative to $m_0(TiO_2)$.

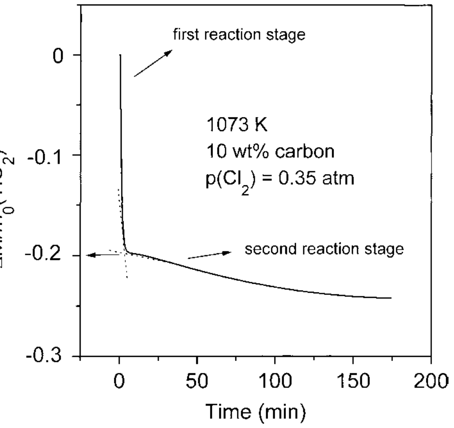

Fig. 2. Total mass change relative to starting oxide mass ($\Delta M/m_0(TiO_2)$) during a typical experiment of carbochlorination. The ordinate of the intersection of the extrapolations of two portions of the curve allows to calculate by Eq. (2), the extention of first stage. In this case $\alpha_\mathrm{f} = 0.15$.

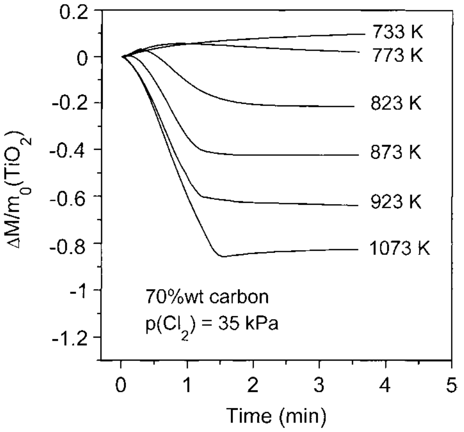

Fig. 3. Total mass change relative to starting oxide mass ($\Delta M/m_0(TiO_2)$) during the first minutes of carbochlorination of TiO_2–70 wt% C mixtures at several temperatures.

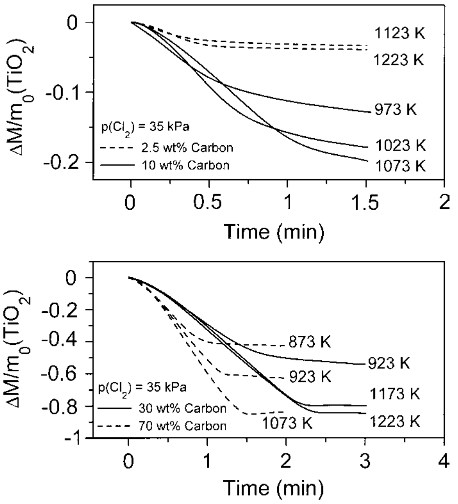

Fig. 4. Effect of temperature on the first reaction stage for several carbon contents.

reaction stage was decreased ($\alpha_f = 0.7$ for 1073 K, $\alpha_f = 0.5$ for 923 K). The reaction rate, $R_{0,f}$, also diminished when the temperature was decreased. Below 873 K, a mass gain was observed initially and increases when the reaction temperature decreased. At 733 K the chlorination of the TiO_2–C mixture reveals mass gain only. Hence, at lower temperatures a net mass gain was the primary effect. At 1073 K during the second reaction stage, a slight mass increase is observed.

Fig. 4 shows the effect of carbon content on the rate of carbochlorination during the first stage at several temperatures. The time zero of thermogravimetric curves illustrated in Fig. 4 differs from that of Fig. 3 and corresponds to the time from which mass loss commenced. Table 1 summarizes the $R_{0,f}$ and α_f

Table 1
Initial reaction rate ($R_{0,f}$) for the first stage of TiO_2 carbochlorination at several carbon contents and temperatures

Carbon content (wt%)	$m_0(TiO_2)$ (mg)	Temperature (K)	$R_{0,f} \times 10^3 (s^{-1})$ (Eq. (3))	$r_{0,f} \times 10^7$ (moles Cl_2/s) (Eq. (4))	α_f
2.5	20.1	1073	0.8	4.0	0.028
2.5	20.0	1123	1.0	5.0	0.022
2.5	24.6	1173	1.1	6.8	0.042
2.5	20.1	1223	1.2	6.0	0.027
10	9.2	973	1.9	4.4	0.101
10	9.0	1023	2.6	5.9	0.146
10	9.2	1073	2.5	5.7	0.153
10	10.2	1173	3.1	7.9	0.102
10	10.0	1223	3.5	8.7	0.103
30	7.2	923	4.5	8.1	0.377
30	7.1	1123	5.3	9.4	0.654
30	7.3	1173	5.4	9.8	0.615
30	9.0	1223	5.4	12.0	0.646
70	3.0	873	6.9	5.2	0.323
70	3.4	923	7.7	6.6	0.461
70	3.1	1073	9.2	7.2	0.661
70	3.4	1223	7.5	6.4	0.673

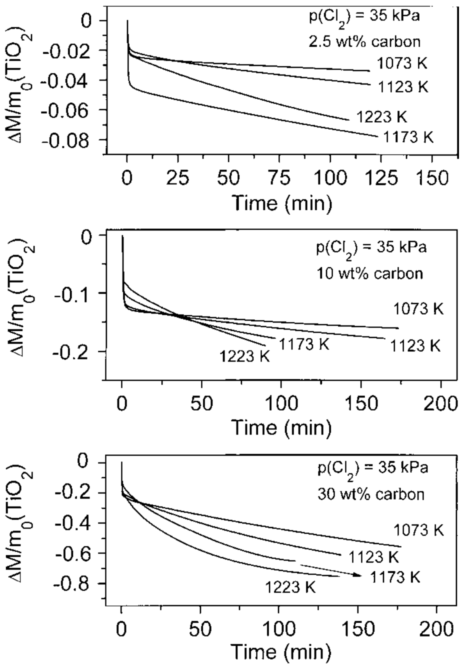

Fig. 5. Effect of temperature on the second reaction stage for several carbon contents.

values. Fig. 4 and Table 1 indicate that, at constant temperature, both $R_{0,\mathrm{f}}$ and α_f increased with increasing carbon fraction.

Fig. 5 shows the effect of temperature upon the second stage for various carbon contents. In Fig. 5 the first stage is also observed in all cases. The second stage was characterized by the initial reaction rate $R_{0,\mathrm{s}}$ which was computed using Eq. (3) from initial slopes of $\Delta M/m_0(\mathrm{TiO_2})$ vs. time curves in Fig. 5, being $m_0(\mathrm{TiO_2})$ the $\mathrm{TiO_2}$ mass when the second stage commenced. The $R_{0,\mathrm{s}}$ values as a function of carbon content and temperature are summarized in Table 2.

One meaningful observation for both reaction stages is that the initial reaction rates ($R_{0,\mathrm{f}}$ and $R_{0,\mathrm{s}}$) increase with carbon content.

3.2. SEM observations

The features of solid powders have been reported in previous works. Carbon is composed of particles with sharp edges and size ranging from less than 1 to 200 μm [16]. $\mathrm{TiO_2}$ powder is composed of hemispherical particles with a size distribution from about 1 up to 60 μm [19].

Fig. 6 shows the features of the particles of initial carbon and $\mathrm{TiO_2}$ powders.

The morphological changes of solids observed during the first reaction stage are well illustrated in Fig. 7. The carbon particle is embedded in the $\mathrm{TiO_2}$ particle. Hence, the $\mathrm{TiO_2}$ particle is strongly attacked in the region closest to the carbon surface, but the carbon particle did not undergo significant attack. The other regions of the $\mathrm{TiO_2}$ particle is unaltered with respect to the particles of the initial powder, indicating that this

Table 2
Initial reaction rate ($R_{0,\mathrm{s}}$) for the second stage of $\mathrm{TiO_2}$ carbochlorination at several carbon contents and temperatures

Carbon content[a] (wt%)	$m_0(\mathrm{TiO_2})$[a] (mg)	Temperature (K)	$R_{0,\mathrm{s}} \times 10^6$ ($\mathrm{s^{-1}}$) (Eq. (3))	$r_{0,\mathrm{s}} \times 10^9$ (moles $\mathrm{Cl_2/s}$) (Eq. (4))
1.7	19.28	1073	3.3	1.6
1.8	19.49	1123	5.0	2.4
0.8	18.93	1173	6.7	3.2
1.7	19.50	1223	12	5.8
7.0	7.7	1023	6.7	1.3
7.7	8.28	1073	12	2.5
7.9	7.99	1123	25	5.0
8.4	9.00	1223	40	9.0
8.0	2.02	1223	130	6.6
8.6	6.57	1223	128	2.1
33.3	0.48	1023	77	0.9
32.4	0.50	1073	147	1.8
32.9	0.57	1123	250	3.6
32.6	0.93	1223	333	7.7

[a] At the beginning of the second stage.

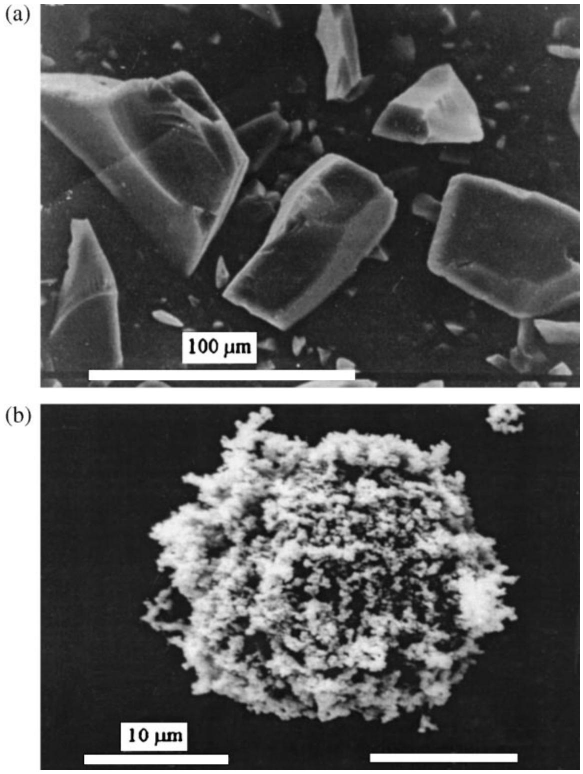

Fig. 6. Particles of the initial (a) carbon and (b) TiO_2 powders.

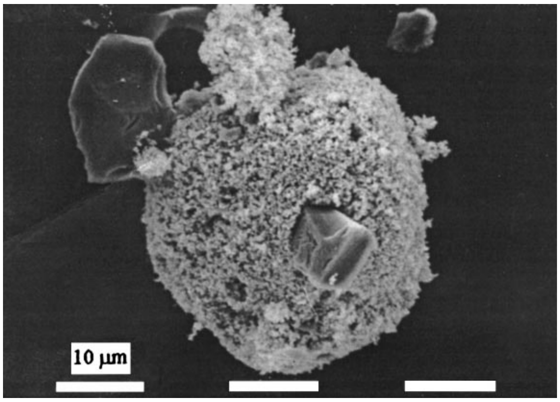

Fig. 7. Effect of localized corrosion on TiO_2 particle during the first reaction stage.

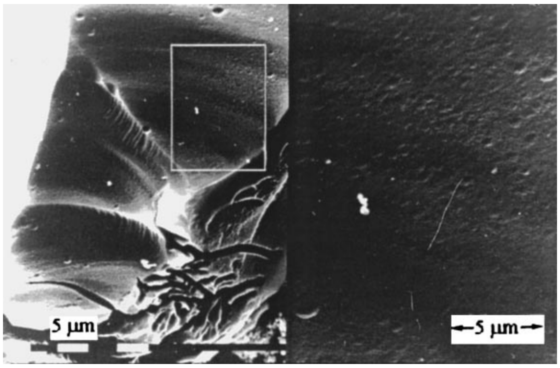

Fig. 8. Effect of localized corrosion on surface carbon particles during the second reaction stage.

interaction with carbon is markedly localized. Most of the TiO_2 particles examined after the first reaction stage were penetrated by carbon particles. It is well known that reduction of TiO_2 by C does not occur [20] and no carbon particles were found penetrating the titanium oxide after being heated in an argon flow [21]. Although the carbon and TiO_2 surfaces are very close, they do not touch. Therefore the chemical attack suffered by TiO_2 particle is not due to reaction directly with carbon. Pasquevich et al. [16] explained this localized effect in ZrO_2 carbochlorination by the formation of very reactive chlorine atoms that reached the oxide surface whenever the distance between these particles was not greater than their mean free path which under equivalent experimental conditions to this work was about 1 µm.

Fig. 8 reveals during the second reaction stage a vigorous chemical attack on carbon particles. TiO_2 particles do not show any differences from the original powder. The carbon particle has undergone a localized corrosion with channellings and cavities. It has been proposed that the C–O_2 reaction in the presence of $ZrCl_4$ and Cl_2 in the gas phase might be the reason for channelling and cracks [16]. The cavities may be created by the effect of the direct contact between particles of TiO_2 resting on the carbon particle. Besides, TiO_2 particles disaggregate during the second reaction stage as shown in Fig. 9. This could facilitate the interaction that produces the carbon corrosion.

Therefore the morphological changes in each reaction stage may be associated with different types of interaction occurring between particles and two distinct reaction mechanisms may operate.

4. Discussion

The carbochlorination is a complex reaction system that can be viewed as a result of some chemical

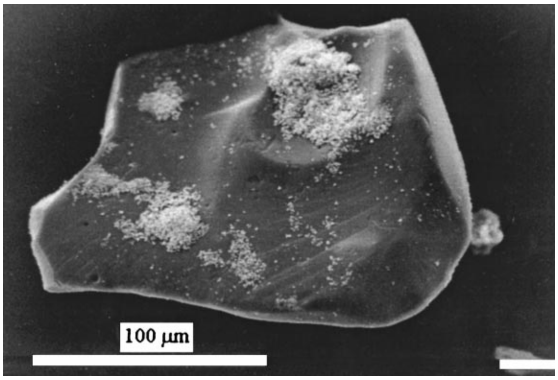

Fig. 9. TiO_2 particle disaggregated over a carbon particle during the second reaction stage.

interaction between the binary gas–solid reactions: C(s)–Cl_2(g) and TiO_2(s)–Cl_2(g). One or both of these could be involved in the formation of active gaseous species that might interact with TiO_2(s) and/or C(s) to form the reaction products.

4.1. C(s)–Cl_2(g) interaction

It is well known that the chlorination of carbon to produce chlorine–carbon gaseous products takes place only above 2273 K [20]. However, at temperatures lower than 1273 K the C–Cl_2 interaction is complex and may involve various phenomena [22]. Physical and chemical adsorption, reaction of chlorine with chemisorbed hydrogen, diffusion and adsorption of chlorine in micropores and dissociation of the chlorine molecule at the carbon surface to form chlorine atoms in the gas phase, have been reported [13]. The mass gain observed when chlorine interacts with carbon (curve (a), Fig. 1) is explained by the following reaction [4,21,22]

$$Cl_2(g) + C^*{-}H(s) \rightarrow HCl(g) + C^*{-}Cl(s), \tag{5}$$

where C^* denotes a surface carbon atom.

4.2. TiO_2(s)–Cl_2(g) interaction

Despite the reaction $TiO_2(s) + Cl_2(g) \rightarrow TiCl_4(g) + O_2(g)$ being thermodynamically unfavourable at the temperature of the experiments, the slow mass loss that takes place during the TiO_2 chlorination (curve (b), Fig. 1) is due to the continuous removal of gaseous products in the Ar–Cl_2 flow.

4.3. TiO_2(s)–C(s)–Cl_2(g) interaction

When the chlorination of TiO_2 is performed in the presence of carbon (curve (c), Fig. 1) a significant mass loss is observed because the carbochlorination (Eq. (1)) is thermodynamically favourable at all temperatures. The mass loss observed above 773 K (Fig. 3) is interpreted from the carbochlorination process (Eq. (1)), whereas at 733 K the net mass gain results from the mass loss of carbochlorination overlapped with the mass gain of C(s)–Cl_2(g) reaction. Therefore, the net mass change observed depends on the relative importance of two phenomena, carbochlorination being the most important at high temperatures. The final mass gain observed in the experiment at 1073 K (Fig. 3) means that after TiO_2 is consumed, interaction of remaining carbon with chlorine occurs. From the results of previous work about ZrO_2–C–Cl_2 system [15] a correction by C(s)–Cl_2(g) reaction was not made.

4.4. Analysis of TiO_2 carbochlorination on the basis of two reaction stages

An important feature to discuss is the transition from the first reaction stage to the second one (Fig. 2). This involved a sudden change in reaction rate similar to the observed instability in ZrO_2 carbochlorination [13,14]. As in the case of ZrO_2 [15], the change is not associated with a consumption of the smallest particles, because the extension of the first step (α_f) depends on the temperature (Fig. 3) and the mass fraction of carbon (Fig. 4) that affect the partial pressure of the reaction intermediates. Hence, each stage of TiO_2 carbochlorination is associated with different mechanisms.

4.5. Controlling regimes

When starvation effects are absent, mass transfer through the boundary layer around the reacting solid can be rate-controlling. In previous work [23] it was determined that in our experimental set-up at 1223 K the mass transfer rate should be between 2×10^{-8} and 2×10^{-7} moles Cl_2/s. When the rate determining step

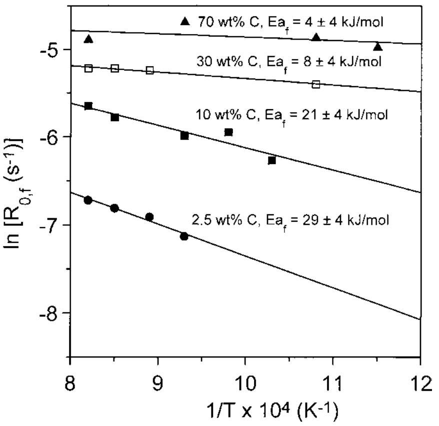

Fig. 10. Computation of activation energies for the first reaction stage.

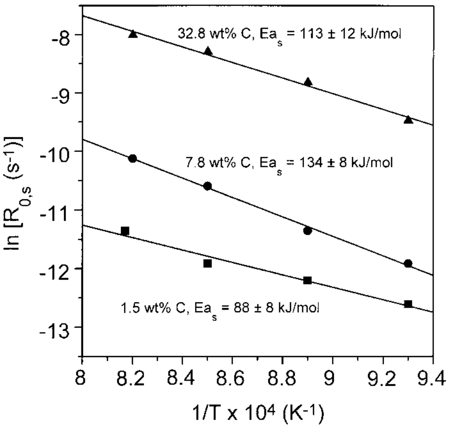

Fig. 11. Computation of activation energies for the second reaction stage. Carbon percentages are average of values of Table 2.

is the diffusion in the gas phase, the reaction rate value r (Eq. (4)) at 1223 K would be within this range.

From the values of reaction rates, $r_{0,\mathrm{f}}$ and $r_{0,\mathrm{s}}$ (Tables 1 and 2), it is observed that external gaseous mass transport influences during the first reaction stage, while the second reaction stage occurs out of the external control. In the case of the first stage the dependence of the reaction rate with the carbon content suggests additional contribution of other controlling regimes. In order to obtain additional criteria, the activation energies associated with both reaction stages were calculated.

Fig. 10 shows ln $R_{0,\mathrm{f}}$ vs. $1/T$ curves for each carbon content constructed from data of Table 1. The corresponding E_a values ($E_\mathrm{af} = 4$–29 kJ mol^{-1}), which are inserted in Fig. 10, are very lower than values associated with a chemically controlled process. Since E_af approaches zero as the carbon content increases, this corroborates that for high carbon percentages the first stage is under external gaseous control [24]. The increase of E_af with the decrease in carbon content indicates that for lower carbon percentages the first stage occurs under internal mixed control.

Fig. 11 shows ln $R_{0,\mathrm{s}}$ vs. $1/T$ curves for each carbon content constructed from data of Table 2. The calculated E_as values, inserted in Fig. 11 are higher than those observed for the first stage. Although, these values are lower than those typical of a process chemically controlled, second stage is mainly chemically controlled. In Table 2, and for 8 wt% of carbon, two experiments performed at 1223 K with lower sample mass were added. The increase in the $R_{0,\mathrm{s}}$ with mass decrease up to a constant value below 7 mg means there are some internal diffusional influence. The increase in $R_{0,\mathrm{s}}$ at 1223 K with the increase in carbon mass fraction is greater than that expected from the mass decrease. Hence, this is due to a carbon effect. Thus carbochlorination changes from a gas diffusion or internal mixed control during the first stage to a mainly chemical control during the second stage. This kinetic instability, as in the case of ZrO_2 carbochlorination [14,15], contrasts with that observed in many gas–solid reactions in which gas diffusion plays a dominant role in controlling the rate at the end of the reaction.

Finally it is well known that the activation energy of a process controlled chemically is twice those of the same process under internal mixed control [24]. In the present case $E_\mathrm{as} > 2E_\mathrm{af}$; hence the mechanisms of both stages are different.

4.6. *Effect of carbon content on carbochlorination rate: kinetic effect*

The interaction between carbon and chlorine could involve, as mentioned, other processes than reaction (5), not necessarily thermogravimetrically detected, with decisive importance for carbochlorination. Taking into account that the increase of carbon content also increases the reaction rate, the kinetic effect based upon the formation of active species at carbon surface is highly probable. Then, the limiting chemical step occurs on the carbon surface. Hence, the kinetic effect of carbon is better observed during the second stage because a chemical control operates.

5. Conclusion

There is a close analogy between ZrO_2 carbochlorination and TiO_2 carbochlorination. The kinetic features of both reactions and the morphological changes undergone by solids are similar. Hence, the fast and slow reaction stages in the ZrO_2 carbochlorination are equivalent to the first and second stages in the TiO_2 carbochlorination, respectively. The same mechanisms operates during the carbochlorination of both oxides. The kinetic instability in both cases involves a transition from a mechanism controlled by mass transfer to a mechanism mainly chemically controlled. Since formation of reaction intermediates (likely chlorine atoms) at the carbon surface is the main chemical process, each reaction stage (fast/first, slow/second) involves a kinetically different intermediates formation. The chemical process does not need a contact of carbon particles with TiO_2 particles during the first reaction stage, but during the second reaction stage such contact could be important.

References

[1] A.J. Kauffman Jr., E. Don Dilling, in: B. Lustman, F. Kerze Jr. (Eds.), Zirconium Production Methods, The Metallurgy of Zirconium, ch. 4, 1st ed., McGraw-Hill, New York, 1955, p. 68.

[2] I. Barin, W. Schuler, Metall. Trans. 11B (1980) 199–206.

[3] S.L. Stefanyuk, I.S. Morozov, Zh. Prikl. Khim. 38 (1965) 737–742.

[4] D.M. Pasquevich, V. Amorebieta, Ber. Bunsenges. Phys. Chem. 96 (1992) 534–541.

[5] P.A. Ramachandran, L.K. Doraiswamy, AIChE J. 28 (1981) 881–900.

[6] A. Landsberg, C.L. Hoatson, F.E. Block, Metall. Trans. 3 (1972) 517–523.

[7] W.E. Dunn Jr, Metall. Trans. 10B (1979) 271–277.

[8] A. Bergholm, Trans. Am. Inst. Min. Engrs. 221 (1961) 1121–1129.

[9] B.K. Chadwick, Y.K. Rao, Trans. Inst. Min. Metall. C 97 (1988) C143–149.

[10] A.K. Galwey, Thermochim. Acta 96 (1985) 259–273.

[11] T. Ishii, T. Tsuchida, R. Furuichi, H. Haga, K. Kudo, Thermochim. Acta 53 (1982) 89–103.

[12] V.T. Amorebieta, A.J. Colussi, Int. J. Chem. Kinet. 17 (1985) 849–858.

[13] D.M. Pasquevich, A. Caneiro, Thermochim. Acta 156 (1989) 275–283.

[14] D.M. Pasquevich, Argentine Patent 317 (1990) 543.

[15] D.M. Pasquevich, Doctoral Thesis, National University of La Plata, 1991.

[16] D.M. Pasquevich, J. Andrade Gamboa, A. Caneiro, Thermochim. Acta 209 (1989) 209–222.

[17] A.E. Bohé, D.M. Pasquevich, Ber. Bunsenges. Phys. Chem. 99 (1995) 553–1558.

[18] J. Szekely, J.W. Evans, H.Y. Sohn, Gas–Solid Reactions, Academic Press, New York, 1976, pp. 109–111.

[19] J. Andrade Gamboa, D.M. Pasquevich, J. Amer. Ceram. Soc. 75(11) (1992) 2934–2938.

[20] J.W. Mellor, A Comprhensive Treatise on Inorganic and Theoretical Chemistry, vol. 4, Longmans, London, 1957, p. 823.

[21] D.M. Pasquevich, Thermochim. Acta 167 (1990) 91–98.

[22] H. Tobias, A. Soffer, Carbon 23 (1985) 281–289.

[23] F.C. Gennari, D.M. Pasquevich, Thermochim. Acta 284 (1996) 325–339.

[24] L.K. Doraiswamy, M.M. Sharma, Heterogeneous Reactions: Analysis, Examples, and Reactor Design, vol. 1, Gas–Solid and Solid–Solid Reactions, Wiley, New York, 1984, pp. 139–140.